# Low-Energy States in $Y^{90}$

YEONG E. KIM
*Lawrence Radiation Laboratory, University of California, Berkeley, California*
(Received 1 April 1963)

The low-energy levels of the odd-odd nucleus $Y^{90}$ are calculated with finite-range central and tensor forces to first order by means of the $j$-$j$ coupled odd-group model. The two-body matrix elements for the central and tensor forces are expressed in the $j$-$j$ representation, from which a generalization to off-diagonal matrix elements is obtained in the limit of the zero range. A phenomenological Gaussian potential without a hard core, estimated from the free two-nucleon potentials of Jackson-Blatt and Brueckner-Gammel-Thaler, is used for the residual interaction. The effects of the tensor force are analyzed in detail as a function of the force range. The numerical results of the calculation are in reasonably good agreement with available experimental spectra.

## I. INTRODUCTION

RECENTLY, an isomeric state in the odd-odd nucleus $Y^{90}$ has been found.[1] It is interesting to see if this isomeric state can be explained in terms of the $j$-$j$ coupling shell model. Furthermore, as several other low-energy states were reported previously,[2] a theoretical calculation of these observed low-energy states is worthwhile, with the hope that it might provide useful information on the effective interaction between protons and neutrons in the nucleus.

We shall adopt the odd-group model with $j$-$j$ coupling in which the nuclear properties of the nucleus are assumed to be determined by the properties of the odd-group particles. In odd-odd nuclei, one assumes that the residual interaction between proton and neutron is sufficiently weak so that it can be considered as a perturbation on the central field of the "nuclear core," and further that the wave function is a vector-coupled product of the wave functions of two odd-group particles.

To justify the theoretical basis of the well-known Nordheim's coupling rule,[3] de-Shalit investigated the case of nuclei with one proton and neutron outside closed shells. He used the zero-range force between them, and obtained expressions for the diagonal matrix elements.[4] Calculations for specific odd-odd nuclei have been made by several workers for the finite-range force in which central exchange forces are included.[5,6]

We shall use the central and tensor parts of the nuclear force, neglecting the spin-orbit force entirely. This practice is probably reasonable, as it appears that the existence of the spin-orbit force in the nuclear force is still questionable. The residual interaction of nucleons outside the closed shell is not well known, and there seem to be no *a priori* reasons for retaining the same strength parameters of the free two-nucleon problem for this interaction. However, because of our ignorance of the exact form of the residual interaction, we shall rely upon the free two-nucleon force parameters in estimating the strengths of our force, which we hope simulates the residual interaction.

## II. ZEROTH-ORDER APPROXIMATION

Before discussing our choice of the residual force between proton and neutron outside closed shells, we describe the basic assumptions that enter into our calculation. In our odd-group model, we assume that the doubly closed shell can be treated as an inert core giving rise to the central field in which nucleons outside the doubly closed shell move. It is assumed that 38 protons and 50 neutrons form closed-shell cores. The assumption that 50 neutrons form a closed shell has been established because $Zr^{90}$ exhibits typical properties of a closed-shell nucleus.[7] The 38-proton subclosed shell has been assumed by several workers,[8] and we make the same assumption. These assumptions simplify the calculation, since there will be only one proton and one neutron outside the doubly closed-shell core in $Y^{90}$. The wave function is then the $j$-$j$-coupled new basis vector, which is a simple vector product of the wave functions of the nonidentical nucleons 1 and 2 (proton and neutron):

$$|a\rangle = R_1(r_1)R_2(r_2)\,|\,j_1 j_2 JM\rangle,$$

where $R_1(r_1)R_2(r_2)$ is the radial part of the wave

* This work was done under the auspices of the U. S. Atomic Energy Commission.

[1] W. L. Alford, D. R. Kochler, and C. E. Mandeville, Phys. Rev. **123**, 1365 (1961); L. Haskin and R. Vandenbosch, *ibid.* **123**, 184 (1961); R. L. Heath, J. E. Cline, C. W. Reich, E. C. Yates, and E. H. Turk, *ibid.* **123**, 903 (1961); W. S. Lyon, J. S. Eldridge, and L. C. Bate, *ibid.* **123**, 1747 (1961).

[2] G. A. Bartholomew, P. J. Campion, J. W. Knowles, and G. Manning, Nucl. Phys. **10**, 590 (1959).

[3] L. W. Nordheim, Phys. Rev. **78**, 294 (1950).

[4] A. de-Shalit, Phys. Rev. **91**, 1479 (1953).

[5] D. Kurath, Phys. Rev. **91**, 1430 (1953); D. M. Brink, Proc. Phys. Soc. (London) **A67**, 757 (1954); S. P. Pandya, Phys. Rev. **108**, 1312 (1957).

[6] N. D. Newby, Jr., and E. J. Konopinski, Phys. Rev. **115**, 434 (1959).

[7] K. W. Ford, Phys. Rev. **98**, 1516 (1955); J. P. Elliot and A. M. Lane, in *Handbuch der Physik*, edited by S. Flügge (Springer-Verlag, Berlin, 1957), Vol. 39, p. 241; R. K. Sheline, Physica **23**, 923 (1957); N. H. Lazar, G. D. O'Kelley, J. H. Hamilton, L. M. Langer, and W. G. Smith, Phys. Rev. **110**, 513 (1958).

[8] B. F. Bayman, A. S. Reiner, and R. K. Sheline, Phys. Rev. **115**, 1627 (1959); V. K. Thankappan and Y. R. Waghmare, Progr. Theoret. Phys. (Kyoto) **22**, 459 (1959); I. Talmi and I. Unna, Nucl. Phys. **19**, 225 (1960); V. K. Thankappan, Y. R. Waghmare, and S. P. Pandya, Progr. Theoret. Phys. (Kyoto) **26**, 22 (1961).

TABLE I. Single-particle levels of the thirty-ninth proton.

| Configuration | Energy (keV) $Y^{89}$ [a] | $Y^{91}$ [a] | $Y^{90}$ [b] |
|---|---|---|---|
| $p_{1/2}$ | 0 | 0 | 0 |
| $g_{9/2}$ | 913 | 551 | 732 |

[a] Experimental data from Ref. 11.
[b] Average between $Y^{89}$ and $Y^{91}$.

function and $|j_1 j_2 JM\rangle$ is the angular part. Now we assume that the Hamiltonian describing this nucleus at low energy may be written as

$$H=H_1+H_2+V_{12},$$

where $H_1$ and $H_2$ are the single-particle shell-model Hamiltonians for particles 1 and 2, respectively, and $V_{12}$ is the two-body interaction between particles 1 and 2. This implies that

$$H_i|a\rangle=\epsilon_0{}^i|a\rangle,$$

for $i=1$ or 2, where $\epsilon_0{}^i$ is the single-particle energy for particle $i$. In the zeroth-order approximation, the level energies are given by the sum of proton and neutron single-particle energies $\sum_i \epsilon_0{}^i$. Estimated single-particle levels have been reported in several works,[9,10] but one cannot avoid the arbitrariness in choosing the parameters involved. Instead, we rely on the experimental single-particle levels of neighboring nuclei to eliminate ambiguity. For the proton single-particle levels, we choose the average values between $Y^{89}$ and $Y^{91}$, and for the neutron single-particle levels the average between $Sr^{89}$ and $Zr^{91}$. The experimental single-particle levels are presented in Tables I and II, and the resulting zeroth-order energy levels are listed in Table III. The assignment for the lowest state of the fifty-first neutron as the $d_{5/2}$ configuration is evident from the fact that the observed ground-state spins and parities of $Sr^{89}$ and $Zr^{91}$ are $\frac{5}{2}^+$.[11] The lowest state of the thirty-ninth proton is assumed to be $p_{1/2}$, since both $Y^{89}$ and $Y^{91}$ are known to have ground-state spin $\frac{1}{2}^-$.[11] Recently, the atomic-beam measurement of the ground-state

TABLE II. Single-particle levels of the fifty-first neutron.

| Configuration | Energy (keV) $Sr^{89}$ [a] | $Zr^{91}$ [b] | $Y^{90}$ [c] |
|---|---|---|---|
| $d_{5/2}$ | 0 | 0 | 0 |
| $s_{1/2}$ | 1050 | 1225 | 1138 |
| $d_{3/2}$ | 2020 | 2070 | 2045 |
| $g_{7/2}$ | ··· | 2205 | 2205 |

[a] Experimental data from B. L. Cohen, Phys. Rev. **125**, 1358 (1962).
[b] Experimental data from Cohen (Ref. a) and Ref. 24.
[c] Average between $Sr^{89}$ and $Zr^{91}$.

[9] S. G. Nilsson, Kgl. Danske Videnskab. Selskab, Mat. Fys. Medd. **29**, No. 16 (1955).
[10] H. Noya, A. Arima, and H. Horie, Suppl. Progr. Theoret. Phys. (Kyoto) **8**, 33 (1958).
[11] D. Strominger, J. M. Hollander, and G. T. Seaborg, Rev. Mod. Phys. **30**, 585 (1958).

TABLE III. The zeroth-order levels in $Y^{90}$.

| Configuration (proton-neutron) | Energy (keV) |
|---|---|
| $p_{1/2}d_{5/2}$ | 0 |
| $g_{9/2}d_{5/2}$ | 732 |
| $p_{1/2}s_{1/2}$ | 1138 |
| $g_{9/2}s_{1/2}$ | 1870 |
| $p_{1/2}d_{3/2}$ | 2045 |
| $p_{1/2}g_{7/2}$ | 2205 |
| $g_{9/2}d_{3/2}$ | 2777 |
| $g_{9/2}g_{7/2}$ | 2937 |

spin has been made for $Y^{91}$, confirming the $p_{1/2}$ configuration.[12] The observed low-energy levels in $Y^{90}$ are shown in Fig. 1. The ground-state spin of $Y^{90}$ has been determined recently by the atomic-beam method to be 2.[13]

We treat $V_{12}$ as a perturbation of the central field of the shell-model core, and evaluate the first-order perturbation term. The total energy for the state of a given $J$ is given approximately then by

$$E\approx\epsilon_0{}^i+\epsilon_1;\quad i=1,2,$$

where the higher terms are neglected. Values for $\epsilon_0{}^i$ are listed in Table III. It is clear that $V_{12}$ removes the degeneracy of the state with various $J$ values arising from a given configuration. The values of $\epsilon_1$, and consequently $E$, are obtained from the eigenvalue equation

$$\sum_{a'}[\langle a|V_{12}|a'\rangle-(E-\epsilon_{0a'}{}^{-1})\delta_{a,a'}]\langle a'|aJM\rangle=0.$$

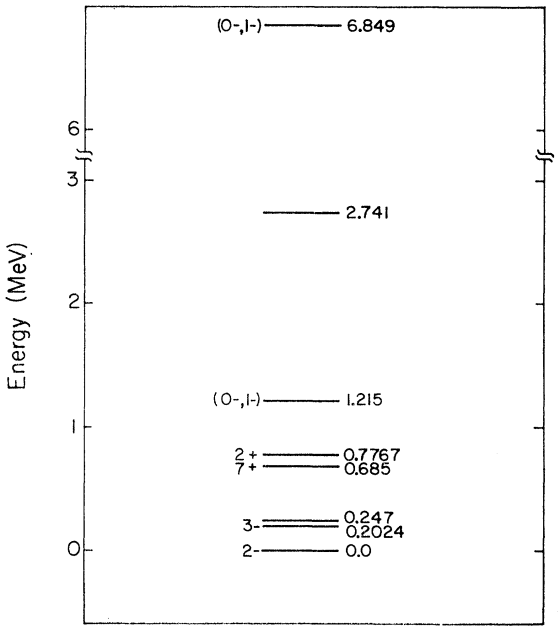


FIG. 1. Experimentally observed low-energy levels in $Y^{90}$.

[12] F. R. Petersen and H. A. Shugart, Phys. Rev. **128**, 1740 (1962).
[13] F. R. Petersen and H. A. Shugart, Phys. Rev. **125**, 284 (1962).

For the numerical calculation, the summation is restricted to the configuration listed in Table III.

### III. RESIDUAL INTERACTION

Now we assume an explicit form of the proton-neutron residual interaction, and proceed to evaluate the matrix element. The residual interaction $V_{12}$ is chosen as

$$V_{12}=V^C(r_{12})+V^T(r_{12})S_{12},$$

where the first term is the central force, and the second term is the tensor force. The explicit forms of these forces are

$$V^C(r_{12})=[V_{\mathrm{TE}}{}^C P_{\mathrm{TE}}\exp(-\beta_{\mathrm{TE}}{}^C r_{12}{}^2)+V_{\mathrm{SE}}{}^C P_{\mathrm{SE}}\times\exp(-\beta_{\mathrm{TE}}{}^C r_{12}{}^2)+V_{\mathrm{TO}}{}^C P_{\mathrm{TO}}\exp(-\beta_{\mathrm{TO}}{}^C r_{12}{}^2)+V_{\mathrm{SO}}{}^C P_{\mathrm{SO}}\exp(-\beta_{\mathrm{SO}}{}^C r_{12}{}^2)],$$

and

$$V^T(r_{12})=V_{\mathrm{TE}}{}^T P_{\mathrm{TE}}\exp(-\beta_{\mathrm{TE}}{}^T r_{12}{}^2)+V_{\mathrm{TO}}{}^T P_{\mathrm{TO}}\exp(-\beta_{\mathrm{TO}}{}^T r_{12}{}^2),$$

where $P_{\mathrm{TE}}$, $P_{\mathrm{SE}}$, $P_{\mathrm{TO}}$, and $P_{\mathrm{SO}}$ are the projection operators for the triplet-even, singlet-even, triplet-odd, and singlet-odd states, respectively, and $V$'s are the corresponding strength parameters. The operator $S_{12}$ is the tensor force operator defined as

$$S_{12}=\frac{3(\boldsymbol{\sigma}_1\cdot\mathbf{r}_{12})(\boldsymbol{\sigma}_2\cdot\mathbf{r}_{12})}{r_{12}{}^2}-\boldsymbol{\sigma}_1\cdot\boldsymbol{\sigma}_2.$$

The matrix element for the central force may be expressed as

$$\langle a|V^C(r_{12})|a'\rangle=\tfrac{1}{2}[(V_{\mathrm{TE}}{}^C+V_{\mathrm{TO}}{}^C)+(V_{\mathrm{TE}}{}^C-V_{\mathrm{TO}}{}^C)(-1)^{j_1'+j_2'+J}P_{12}']\langle a|U^C(r_{12})|a'\rangle-\tfrac{1}{2}[(V_{\mathrm{TE}}{}^C-V_{\mathrm{SE}}{}^C+V_{\mathrm{TO}}{}^C-V_{\mathrm{SO}}{}^C)+(V_{\mathrm{TE}}{}^C+V_{\mathrm{SE}}{}^C-V_{\mathrm{TO}}{}^C-V_{\mathrm{SO}}{}^C)(-1)^{j_1'+j_2'+J}P_{12}']\times\langle a|U^C(r_{12})P_S|a'\rangle,$$

where $P_S$ is the singlet projection operator, and $P_{12}'$ is an exchange operator which interchanges $l_1'\leftrightarrow l_2'$ and $j_1'\leftrightarrow j_2'$ in the primed (initial) states. The matrix elements $\langle a|U^C(r_{12})|a'\rangle$ and $\langle a|U^C(r_{12})P_S|a'\rangle$ are given by (see Appendix A)

$$\langle a|U^C(r_{12})|a'\rangle=(-1)^{j_2'+j_2+J}([j_1][j_2][j_1'][j_2'])^{1/2}\sum_k F_k(j_1'\tfrac{1}{2}j_1-\tfrac{1}{2}|k0)(j_2'\tfrac{1}{2}j_2-\tfrac{1}{2}|k0)W(j_1j_1'j_2j_2';kJ),$$

$$\langle a|U^C(r_{12})P_S|a'\rangle=(-1)^{j_2'+j_2+J+1}([j_1][j_2][j_1'][j_2'])^{1/2}([l_1][l_2][l_1'][l_2'])^{1/2}W(l_1j_1l_2j_2;\tfrac{1}{2}J)\times W(l_1'j_1'l_2'j_2';\tfrac{1}{2}J)\sum_k F_k(l_10l_1'0|k0)(l_20l_2'0|k0)W(l_1l_1'l_2l_2';kJ),$$

and with the restriction that $k+l_1+l_1'$ and $k+l_2+l_2'$ are both even. The symbol $[a]$ stands for $[2a+1]$, and $(\ |\ )$ and $W$ are the usual Clebsch-Gordan and Racah coefficients. The Slater integral $F_k$ is defined as

$$F_k=\int_0^\infty dr_1\, r_1{}^2R_1R_1'\int_0^\infty dr_2\, r_2{}^2R_2R_2'\times\int_{-1}^{1}d\left(\frac{\cos\theta_{12}}{2}\right)P_k(\cos\theta_{12})U^C(r_{12}),$$

where $U^C(r_{12})$ takes the Gaussian form $\exp(-\beta r_{12}{}^2)$ with different values of $\beta$ for the corresponding states.

For the tensor force, the matrix element can be expressed as

$$\langle a|V^T(r_{12})S_{12}|a'\rangle=\tfrac{1}{2}[(V_{\mathrm{TE}}{}^T+V_{\mathrm{TO}}{}^T)+(V_{\mathrm{TE}}{}^T-V_{\mathrm{TO}}{}^T)(-1)^{j_1'+j_2'+J}P_{12}']\langle a|U^T(r_{12})S_{12}|a'\rangle,$$

and (see Appendix B)

$$\langle a|U^T(r_{12})S_{12}|a'\rangle=3\sum_{K,x,y}\langle\alpha|F_{xy}|\alpha'\rangle W(1x1y;K2)\times\langle j_1j_2JM|\mathbf{T}_1{}^{(1x)K}\cdot\mathbf{T}_2{}^{(1y)K}|j_1'j_2'JM\rangle,$$

where

$$\langle\alpha|F_{xy}|\alpha'\rangle=-5\sum_{k,i,j}\langle\alpha|r_ir_j|\alpha'\rangle X_{ij},\quad i,j=1,2;$$

$$X_{11}=(2/15)^{1/2}[x]^{1/2}(20k0|x0),$$

$$X_{22}=(2/15)^{1/2}[y]^{1/2}(20k0|y0),$$

$$X_{12}=([x][y])^{1/2}(10k0|x0)(10k0|y0)\times W(11xy;2k),$$

and

$$\langle\alpha|r_ir_j|\alpha'\rangle=(2k+1)\int_0^\infty dr_1\, r_1{}^2R_1R_1'\int_0^\infty dr_2\, r_2{}^2R_2R_2'r_ir_j\times\int_{-1}^{1}d\left(\frac{\cos\theta_{12}}{2}\right)P_k(\cos\theta_{12})\frac{U^T(r_{12})}{r_{12}{}^2}.$$

Here the form of the radial function for the triplet-even state is

$$U^T(r_{12})=\exp(-\beta_{\mathrm{TE}}{}^T r_{12}{}^2),$$

and for the triplet-odd state,

$$U^T(r_{12})=\exp(-\beta_{\mathrm{TO}}{}^T r_{12}{}^2).$$

The angular part in terms of 3-, 6-, and 9-$j$ symbols is

$$\langle j_1j_2JM|\mathbf{T}_1{}^{(1x)K}\cdot\mathbf{T}_2{}^{(1y)K}|j_1'j_2'J'M'\rangle=(-1)^{j_1'+j_2+l_1+l_2+J}6\delta_{JJ'}\delta_{MM'}\begin{Bmatrix}J & j_2 & j_1\\ K & j_1' & j_2'\end{Bmatrix}([j_1][j_2][j_1'][j_2'])^{1/2}\times([l_1][l_2][l_1'][l_2'])^{1/2}\begin{pmatrix}l_1 & x & l_1'\\ 0 & 0 & 0\end{pmatrix}\begin{pmatrix}l_2 & y & l_2'\\ 0 & 0 & 0\end{pmatrix}\begin{Bmatrix}\frac{1}{2} & \frac{1}{2} & 1\\ l_1' & l_1 & x\\ j_1' & j_1 & K\end{Bmatrix}\begin{Bmatrix}\frac{1}{2} & \frac{1}{2} & 1\\ l_2' & l_2 & y\\ j_2' & j_2 & K\end{Bmatrix}.$$

In the zero range, the tensor force vanishes, and the central force matrix element reduces to

$$\langle a|V^C(r_{12})|a'\rangle \rightarrow (4\pi)^{-1}\left(\frac{\pi}{\beta}\right)^{3/2} \times[(3V_{\mathrm{TE}}{}^C+V_{\mathrm{SE}}{}^C)\langle a|\delta(\mathbf{r}_1-\mathbf{r}_2)|a'\rangle + (V_{\mathrm{TE}}{}^C-V_{\mathrm{SE}}{}^C)\langle a|\delta(\mathbf{r}_1-\mathbf{r}_2)\boldsymbol{\sigma}_1\cdot\boldsymbol{\sigma}_2|a'\rangle],$$

where (see Appendix A)

$$\langle a|\delta(\mathbf{r}_1-\mathbf{r}_2)|a'\rangle=(1/2[J])F_0([j_1][j_2][j_1'][j_2'])^{1/2} \times(j_1\tfrac{1}{2}j_2-\tfrac{1}{2}|J0)(j_1'\tfrac{1}{2}j_2'-\tfrac{1}{2}|J0) \times\left[(-1)^{j_1+j_1'+l_1+l_1'+1}+(-1)^{j_1+j_1'+j_2+j_2'}\frac{AA'}{4J(J+1)}\right],$$

and

$$\langle a|\delta(\mathbf{r}_1-\mathbf{r}_2)\boldsymbol{\sigma}_1\cdot\boldsymbol{\sigma}_2|a'\rangle =(1/2[J])F_0([j_1][j_2][j_1'][j_2'])^{1/2} \times(j_1\tfrac{1}{2}j_2-\tfrac{1}{2}|J0)(j_1'\tfrac{1}{2}j_2'-\tfrac{1}{2}|J0) \times\left\{(-1)^{j_1+j_1'+l_1+l_1'}[1+2(-1)^{l_1+l_2+J}] +(-1)^{j_1+j_1'+j_2+j_2'}\frac{AA'}{4J(J+1)}\right\},$$

with

$$A=[(2j_1+1)+(-1)^{j_1+j_2+J}(2j_2+1)].$$

The matrix element $\langle a|V^0(r_{12})\boldsymbol{\sigma}_1\cdot\boldsymbol{\sigma}_2|a'\rangle$ vanishes unless both $l_1+l_2+J$ and $l_1'+l_2'+J$ are even. Similarly, $\langle a|V^0(r_{12})|a'\rangle$ vanishes unless $l_1+l_1'+l_2+l_2'$ is even. The Slater integral $F_0$ is given by

$$F_0=\int_0^\infty R_1(r)R_2(r)R_1'(r)R_2'(r)r^2dr.$$

For the radial part of the wave function, we choose the harmonic-oscillator wave function. It is generally believed that the harmonic-oscillator wave function is a fairly good approximation for light and medium nuclei, whereas the square-well potential is a closer approximation for heavy nuclei. The radial wave function has the explicit form[14]

$$R_{nl}(r)=N_{nl}e^{-(\nu/2)r^2}r^l v_{nl}(r),$$

where $N_{nl}$ is a normalization constant chosen so that

$$\int R_{nl}{}^*(r)R_{nl}(r)r^2dr=1.$$

The function $v_{nl}(r)$ is the associated Laguerre polynomial defined as

$$v_{nl}(r)=L_{n+l+1/2}{}^{l+1/2}(\nu r^2) =\sum_{k=0}^{n}(-1)^k 2^k\binom{n}{k}\frac{(2l+1)!!}{(2l+k+1)!!}(\nu r^2)^k.$$

The nuclear size parameter $\nu^{-1/2}$ appearing in the wave function has to be evaluated for the numerical calculation. The harmonic-oscillator spacing is known to be roughly

$$\hbar\omega=\hbar^2\nu/m\cong 41A^{-1/3}\ \mathrm{MeV},$$

from which $\nu$ may be evaluated. The evaluation of the central-force radial integral has been simplified analytically by Ford and Konopinski.[15] The tensor-force radial integral $\langle\alpha|r_ir_j|\alpha'\rangle$ cannot be evaluated directly, since the integral has singularities due to the $r_{12}{}^2$ term appearing in the denominator. This difficulty is eliminated by expanding the integral into a linear combination of the Talmi integral.[14,15] (See Appendix B.) For the delta-function force, the radial integral can be easily evaluated analytically, and the numerical values of the integral have been given by several workers for the diagonal case.[11,16]

## IV. ENERGY SPECTRUM

Before introducing the tensor force, the numerical calculations are carried out extensively with various central force mixtures including Serber, Ferrell-Visscher, and Rosenfeld forces and with various ranges. Although the delta-function force may give the correct sequence of the observed levels in $Y^{90}$ as shown by Bouten *et al.*,[17] the calculations with realistic finite-range forces indicate that we must introduce a fairly strong attractive odd force to fit the experimental data if we were to retain the singlet-even to triplet-even ratio ($\sim$0.5) of the free two-nucleon potential. A calculation with one set of central-force parameters with rather strong attractive odd forces, which is chosen so as to fit both the doublet spacings of $J=2-$, $3-$ and $J=2+$, $7+$, is shown in Fig. 2. Although the fit with the experiment is good, there is no justification for assuming the central force mixture of strong attractive odd force. Furthermore, this is not the only set of parameters which gives rise to a good fit with the experiment, since there are other sets of the parameters which yield equally good fits. From the free two-nucleon potential, it is known that the triplet-odd force is weak, and the singlet-odd is even repulsive.

To include the tensor force in the residual interaction, we must decide the strength of the tensor force. Since the relative weight of the central and tensor force is

[14] I. Talmi, Helv. Phys. Acta 25, 185 (1952).

[15] K. W. Ford and E. J. Konopinski, Nucl. Phys. 9, 218 (1958/59).

[16] N. Zeldes, Nucl. Phys. 2, 1 (1956/57).

[17] M. Bouten, M. Demeur, and H. Pollak, J. Phys. Radium 22, 697 (1961).

TABLE IV. Values of the intrinsic range and well-depth parameters, $s$ and $b$, for the BGT and simulated BGT potentials. The intrinsic ranges for the simulated BGT potential are assumed to be same as the BGT potential and are not shown. The corresponding strength and force range parameters for the simulated BGT are also shown.

| States | BGT $s$ | BGT $b$(F) | Simulated BGT $s$ | Simulated BGT Strength (MeV) | Simulated BGT Force range (F) |
|---|---|---|---|---|---|
| Central triplet-even | 2.882 | 1.013 | 1.0 | −223.02 | 0.706 |
| Central singlet-even | 2.964 | 1.461 | 1.028 | −110.03 | 1.018 |
| Central triplet-odd | 0.201 | 2.119 | 0.070 | −3.57 | 1.476 |
| Central singlet-odd | −1.867 | 2.119 | −0.648 | +33.06 | 1.476 |
| Tensor triplet-even | 2.078 | 2.019 | 0.721 | −40.50 | 1.407 |
| Tensor triplet-odd | −0.493 | 2.649 | −0.171 | +5.58 | 1.845 |

not well known in the residual force, we use the free two-nucleon potential to estimate the tensor-force parameters. Recent success of $O^{18}$ calculations by Dawson, Talmi, and Walecka[18] encourages us to try the Brueckner-Gammel-Thaler potential, hereafter abbreviated BGT.[19] Because of the computational complexity involved, we take a form of the potential different from the BGT. We modify the Yukawa radial dependence with a hard core of the BGT potential by replacing it with the Gaussian radial function neglecting the hard core.

In estimating the strengths and ranges of our Gaussian potential without a hard core, we use the detailed analysis of Blatt and Jackson for the free proton-neutron system in the shape-independent approximation.[20] If one considers a nuclear potential of $V(r)=sV'(r)$ so that $V'(r)$ is the potential that gives rise to zero-binding energy for the ground state of the proton-neutron system, then $V(r)$ for $s>1$ allows bound states, whereas $V(r)$ for $s<1$ gives rise to virtual states. The intrinsic range $b$ of $V(r)$ is then defined as the effective range of $V'(r)$, and $s$ is called the well-depth parameter. The Yukawa and Gaussian potentials in the shape-independent approximation are expressed by Blatt and Jackson in terms of $s$ and $b$ as

$$-V(r)=s(147.585\ \text{MeV})b^{-2}(b/r)\exp[-2.1196(r/b)]$$

for the Yukawa potential, and

$$-V(r)=s(229.208\ \text{MeV})b^{-2}\exp[-2.0604(r/b)^2]$$

for the Gaussian potential, where $b$ is in units of $10^{-13}$ cm.

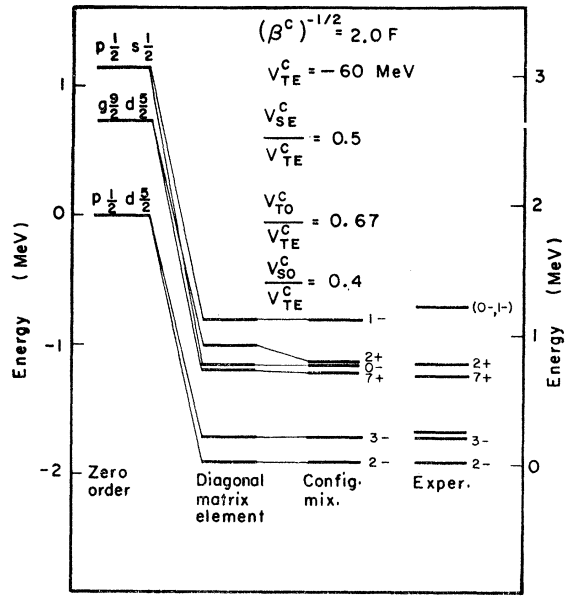


FIG. 2. Calculated $Y^{90}$ spectrum with the central force alone. The central-force parameters are adjusted to fit both the doublet spacings of $J=2$, 3− and $J=2+$, 7+.

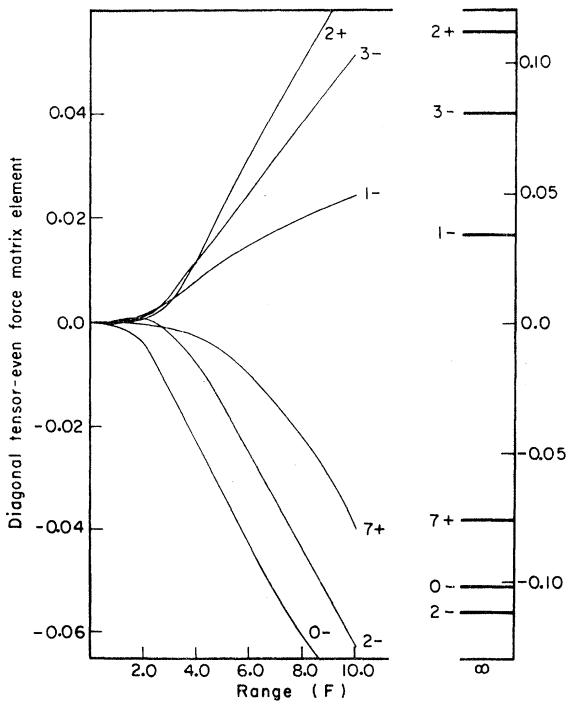


FIG. 3. Diagonal tensor-even-force matrix elements for several observed states in $Y^{90}$ as a function of the range parameter.

[18] J. F. Dawson, I. Talmi, and J. D. Walecka, Ann. Phys. (N. Y.) 18, 339 (1962).
[19] K. A. Brueckner and J. L. Gammel, Phys. Rev. 109, 1023 (1958).
[20] J. M. Blatt and J. D. Jackson, Phys. Rev. 76, 18 (1949).

The introduction of a hard core always makes the force range shorter and the well deeper. However, we retain the intrinsic ranges of the BGT potential for our simulated potential of the Gaussian form, and adjust the well-depth parameters so as to be consistent with the low-energy properties of the deuteron. The well-depth parameters are normalized to the triplet-even part of the central potential, which has been reduced from $s=2.88$ of the BGT potential to $s=1$. Then the triplet-even part of the simulated BGT thus, obtained fits approximately the ground-state and low-energy properties of the deuteron (the binding energy, quadrupole moment, percentage of $D$ state, and triplet scattering length).[21] The values of the parameters $s$ and $b$ for the BGT and simulated BGT are listed in Table IV.

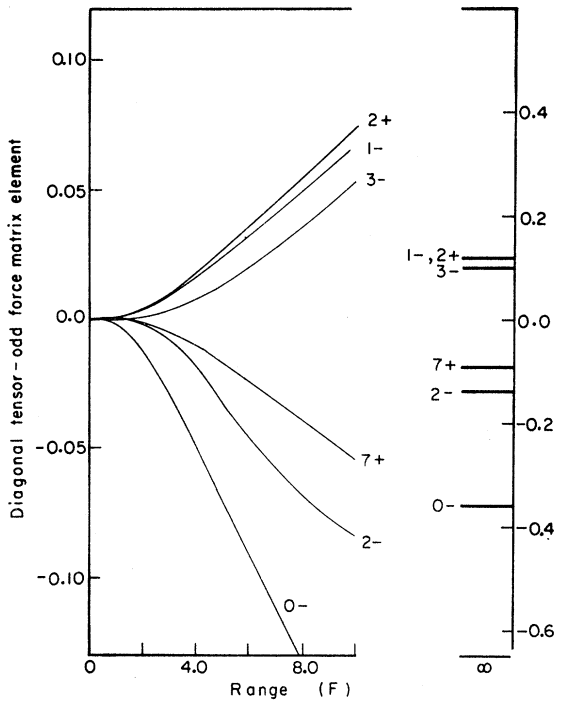


FIG. 4. Diagonal tensor-odd-force matrix elements for several observed states in $Y^{90}$ as a function of the range parameter.

The diagonal tensor-force matrix elements

$$(1/3)\langle a|P_{\mathrm{TE}}U^{T}(r_{12})S_{12}|a\rangle$$

and

$$(1/3)\langle a|P_{\mathrm{TO}}U^{T}(r_{12})S_{12}|a\rangle$$

are plotted as a function of the range in Figs. 3–5. As we can see from these figures, the tensor-force matrix elements are not always a monotonically increasing function of the range, and may be either positive or negative. This is to be contrasted with the fact that the central-force matrix elements are positive and monotonically increasing functions with increasing range and constant depth. The results of the calculation with the simulated BGT potential are compared with the experiment in Fig. 6. In diagonalizing the matrix, the off-diagonal tensor-force matrix elements are neglected, since they are small compared to the diagonal tensor-force matrix elements. The numerical results are also presented in Table V, and are shown schematically in Fig. 7. In Fig. 7, notice that the lowest and highest $J$ states (2+ and 7+) are separated from the other $J$ states arising from the same configuration, $g_{9/2}d_{5/2}$. This is consistent with the revised "weak" coupling rule of Brennan and Bernstein.[22]

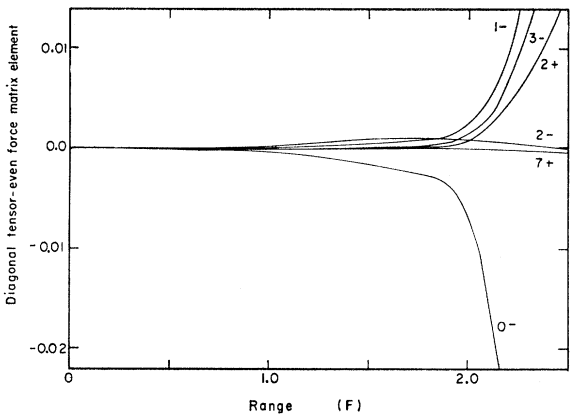


FIG. 5. Diagonal tensor-even-force matrix elements for the observed states in $Y^{90}$ as a function of the range at the shorter ranges.

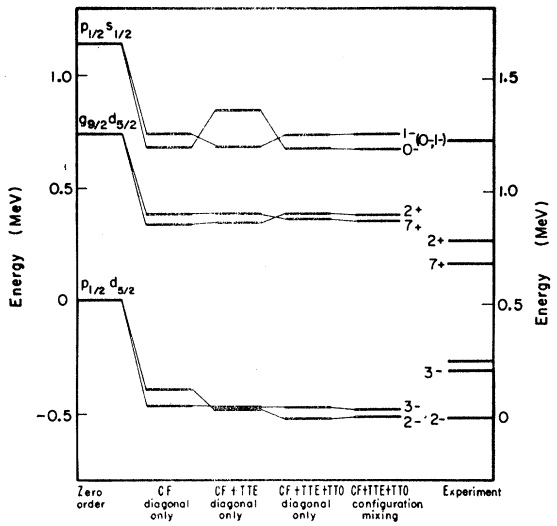


FIG. 6. Comparison of the experimental and calculated spectra of $Y^{90}$ with the simulated BGT potential. The symbols CF, TTE, and TTO stand for the central, tensor-even, and tensor-odd forces, respectively. In diagonalizing the matrix, the off-diagonal matrix elements for the tensor force are neglected.

[21] M. H. Kalos, L. C. Biedenharn, and J. M. Blatt, Nucl. Phys. **1**, 233 (1956).

[22] M. H. Brennan and A. M. Bernstein, Phys. Rev. **120**, 927 (1960).

TABLE V. Calculated energy levels in $Y^{90}$. The results before and after diagonalization are shown in columns A and B, respectively. In column C, the energy scale is shifted so that the ground state lies at zero energy. In diagonalizing, the matrix the tensor-force off-diagonal matrix elements are neglected.

| Proton-neutron configurations | $J\pi$ | Energy (MeV) A | B | C |
|---|---|---|---|---|
| $p_{1/2}d_{5/2}$ | 2− | −0.515 | −0.516 | 0.0 |
| | 3− | −0.480 | −0.487 | 0.029 |
| $g_{9/2}d_{5/2}$ | 2+ | 0.382 | 0.377 | 0.893 |
| | 3+ | 0.622 | 0.600 | 1.116 |
| | 4+ | 0.624 | 0.610 | 1.126 |
| | 5+ | 0.583 | 0.551 | 1.067 |
| | 6+ | 0.679 | 0.679 | 1.195 |
| | 7+ | 0.359 | 0.357 | 0.873 |
| $p_{1/2}s_{1/2}$ | 0− | 0.672 | 0.672 | 1.188 |
| | 1− | 0.734 | 0.734 | 1.250 |
| $g_{9/2}s_{1/2}$ | 4+ | 1.736 | 1.745 | 2.261 |
| | 5+ | 1.655 | 1.671 | 2.187 |
| $p_{1/2}d_{3/2}$ | 1− | 1.815 | 1.816 | 2.332 |
| | 2− | 1.650 | 1.650 | 2.166 |
| $p_{1/2}g_{7/2}$ | 3− | 2.047 | 2.054 | 2.570 |
| | 4− | 1.927 | 1.927 | 2.443 |
| $g_{9/2}d_{3/2}$ | 3+ | 2.372 | 2.326 | 2.842 |
| | 4+ | 2.609 | 2.686 | 3.202 |
| | 5+ | 2.677 | 2.671 | 3.187 |
| | 6+ | 2.487 | 2.663 | 3.179 |
| $g_{9/2}g_{7/2}$ | 1+ | 1.669 | 1.669 | 2.185 |
| | 2+ | 2.269 | 2.274 | 1.753 |
| | 3+ | 2.615 | 2.683 | 3.199 |
| | 4+ | 2.491 | 2.420 | 2.936 |
| | 5+ | 2.769 | 2.790 | 3.306 |
| | 6+ | 2.470 | 2.295 | 2.811 |
| | 7+ | 2.841 | 2.842 | 3.358 |
| | 8+ | 2.129 | 2.129 | 2.645 |

The results of other configurations presented in Fig. 7 and Table V are also consistent with coupling rules of Nordheim,[3] and de-Shalit and Walecka.[23] The eigenfunctions are also computed, and the results are shown in Tables VI and VII. As we can see from these tables, the configuration mixing is not very important for most of the observed states. The almost pure configuration of the ground state $(p_{1/2}d_{5/2})^{J=2-}$ is consistent with the measured magnetic moment. The measured magnetic moment of the ground state of $Y^{90}$ is −1.629 nm, whereas the calculated magnetic moment with the empirical $g$ factors evaluated from neighboring nuclei is −1.609 nm if we assume that the configuration is pure.[13] A level at 0.247 MeV has been suggested by

TABLE VI. Calculated eigenfunctions for odd-parity states in $Y^{90}$.

| $J\pi$ | Eigenvalues (MeV) | Eigenfunctions $p_{1/2}d_{5/2}$ | $p_{1/2}s_{1/2}$ | $p_{1/2}d_{3/2}$ | $p_{1/2}g_{7/2}$ |
|---|---|---|---|---|---|
| 1− | 0.734 | | 0.9997 | 0.0246 | |
| | 1.816 | | 0.0246 | −0.9997 | |
| 2− | −0.516 | −0.9998 | | 0.0158 | |
| | 1.650 | −0.0158 | | −0.9998 | |
| 3− | −0.487 | 0.9987 | | | 0.0500 |
| | 2.054 | 0.0500 | | | −0.9987 |

[23] A. de-Shalit and J. D. Walecka, Nucl. Phys. **22**, 184 (1961).

TABLE VII. Calculated eigenfunctions for even-parity states in $Y^{90}$.

| $J\pi$ | Eigenvalues (MeV) | Eigenfunctions $g_{9/2}d_{5/2}$ | $g_{9/2}s_{1/2}$ | $g_{9/2}d_{3/2}$ | $g_{9/2}g_{7/2}$ |
|---|---|---|---|---|---|
| 2+ | 0.377 | 0.9987 | | | 0.0491 |
| | 2.274 | 0.0491 | | | −0.9987 |
| 3+ | 0.600 | −0.9937 | | 0.1070 | 0.0332 |
| | 2.326 | −0.1108 | | −0.8962 | −0.4294 |
| | 2.683 | −0.0161 | | −0.4304 | 0.9024 |
| 4+ | 0.610 | 0.9938 | 0.1100 | 0.0079 | −0.0040 |
| | 1.745 | 0.1101 | −0.9906 | −0.0736 | −0.0314 |
| | 2.420 | 0.0064 | −0.0648 | 0.5174 | 0.8532 |
| | 2.686 | 0.0037 | 0.0472 | −0.8524 | 0.5206 |
| 5+ | 0.551 | 0.9860 | 0.1578 | −0.0466 | −0.0248 |
| | 1.671 | 0.1623 | −0.9871 | 0.0949 | 0.0295 |
| | 2.671 | 0.0361 | 0.1060 | 0.9105 | 0.3980 |
| | 2.790 | 0.0058 | −0.0100 | −0.3997 | 0.9165 |
| 6+ | 0.679 | 0.9997 | | −0.0115 | −0.0174 |
| | 2.295 | 0.0206 | | 0.6906 | 0.7229 |
| | 2.663 | 0.0037 | | −0.7231 | 0.6907 |
| 7+ | 0.357 | −0.9996 | | | 0.0263 |
| | 2.842 | −0.0263 | | | −0.9996 |

Bartholomew *et al.*[2] to be the $J=3-$ state arising from the $p_{1/2}g_{7/2}$ configuration. They have indicated that this assignment is consistent with their data and with the observed beta decay of $Sr^{90}$ (total disintegration energy of 0.535 MeV) only to the ground state, thus, eliminating the possibility of this state being $J=\pm 0$, $1\pm$, or $2-$. However, the $g_{7/2}$ neutron single-particle level has been found [24] to be 2.2 MeV above the ground state $d_{5/2}$ in $Zr^{91}$, and it is very difficult to understand the $(p_{1/2}g_{7/2})^{J=3}$ state being near the ground state. This would require an extremely large matrix element to over come this initial neutron single-particle spacing of 2.2 MeV. The low energy of 0.247 MeV suggests that this level is probably not attributable to the configuration $(p_{1/2}g_{9/2})$ nor other configurations caused by the core excitation of the 38-proton core. It remains to be seen if the experiment can definitely assign the spin and parity to this state.

The spin and parity of the state at 2.7 MeV have not been determined experimentally, and there are several calculated levels around 2.7 MeV. The probable states within the energy limit of 2.7±0.2 MeV are $(p_{1/2}g_{5/2})^{J=3,4}$, $(g_{9/2}d_{3/2})^{J=3}$, and $(g_{9/2}g_{7/2})^{J=2,6,8}$.

## V. DISCUSSION

Some shell-model and nuclear-matter calculations have indicated that the nuclear force inside the nucleus is not very much different from the free two-nucleon potential. Our approach was that the residual interaction could be approximated by the free two-nucleon potential. Because of enormous complexity arising from the introduction of a hard core, we have neglected the hard core and used a phenomenological Gaussian potential which is deduced from the free two-nucleon

[24] R. L. Preston, H. J. Martin, Jr., and M. B. Sampson, Phys. Rev. **121**, 1741 (1961).

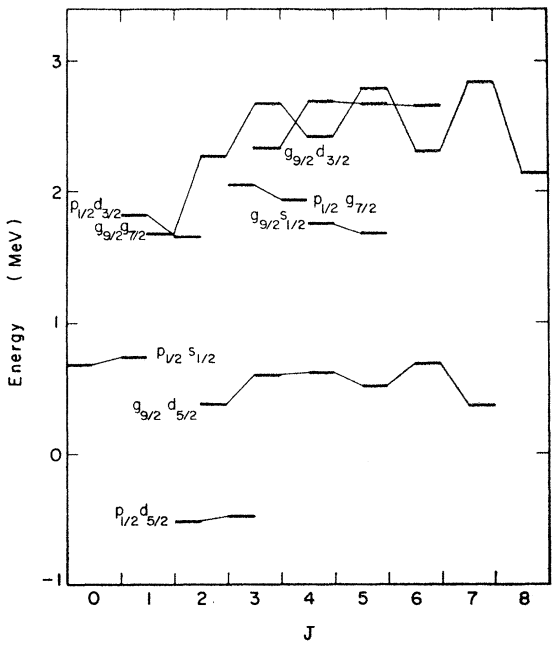


FIG. 7. Calculated energy levels in $Y^{90}$. For each spin, the left-hand column gives the odd-parity states and the right-hand column the even-parity states. Various $J$ states arising from the same configuration are connected by thin lines.

potentials of Jackson-Blatt and Brueckner-Gammel-Thaler. Although the experimental spectrum is not sufficiently resolved to indicate that our choice of the residual force is good, there is a remarkable agreement between the calculated spectrum and experiment if one notes that several shell-model approximations have been made and the force parameters are not all adjusted arbitrarily. A slight increase of the triplet-even part of the central and tensor forces is sufficient to increase the doublet spacings of $J=2-$, $3-$, and $J=2+$, $7+$ so as to improve agreement with experiment. Furthermore, by introducing the tensor force, we can eliminate the unrealistic strong attractive odd central forces. Concurrently, the simulated BGT potential is used for $Bi^{210}$,[25] where most levels of the ground-state multiplet (total of nine levels out of possible ten) are resolved by the high-resolution $(d,p)$ reaction on $Bi^{209}$ at the Massachusetts Institute of Technology.[26] The analysis of those multiplets in $Bi^{210}$ along with $Po^{210}$ also indicates that the triplet-even part of the simulated BGT potential is slightly too weak to account for the over-all spacings of the $Bi^{210}$ ground-state multiplet. A slight increase of the triplet-even part of the simulated BGT potential improves the spacing of $J=2-$, $3-$ states. It would be very interesting to see if one can resolve $g_{9/2}d_{5/2}$ and $p_{1/2}s_{1/2}$ configurations by using the high-resolution $Y^{89}(d,p)Y^{90}$, $Zr^{91}(\alpha,t)Nb^{92}$, or $Zr^{90}(\alpha,d)Nb^{92}$ reactions.

Finally, we should comment on the shell-model residual interaction. From the analysis of various shell-model calculations, the central force alone seems to approximate the residual force very well in most cases, though many of these cases involve like nucleons, where the Pauli principle makes the tensor-even force inoperative. However, the tensor-force contributions are not always negligible, and must be taken seriously in some cases such as in $Y^{90}$ presented here. The characteristic of the tensor-force matrix element is that it may be either positive or negative, so that in some cases the tensor force effects cannot be exactly simulated by a linear combination of four central force components. Also, it should be noted that it is very difficult to simulate the finite-shorter-range tensor force by adjusting the strength parameters of the infinite-range tensor force and that the infinite-range approximation for the tensor force is quite unreliable.

## ACKNOWLEDGMENTS

I am greatly indebted to Dr. Norman K. Glendenning, Dr. Hans J. Mang, and Professor John O. Rasmussen for their advice during the course of this work. I also express my gratitude to Professor Rasmussen for reading the manuscript. The computational work was performed on the IBM-7090 computer at the Lawrence Radiation Laboratory, Berkeley, California.

## APPENDIX A

Our interest here is to evaluate the spin-dependent part of the central-force matrix element

$$\langle a|V(r_{12})\boldsymbol{\sigma}_1\cdot\boldsymbol{\sigma}_2|a\rangle.$$

It is convenient to consider the singlet projection operator $P_S$ and write the matrix element of $V(r_{12})P_S$,

$$\langle a|V(r_{12})P_S|a'\rangle=\tfrac{1}{4}\langle a|V(\mathbf{r}_1-\mathbf{r}_2)(1-\boldsymbol{\sigma}_1\cdot\boldsymbol{\sigma}_2)|a'\rangle. \quad \text{(A1)}$$

Here, $V(\mathbf{r}_1-\mathbf{r}_2)$ can be expanded in terms of the angle $\omega$ between $\mathbf{r}_1$ and $\mathbf{r}_2$

$$V(\mathbf{r}_1-\mathbf{r}_2)=\sum_k v_k(r_1,r_2)P_k(\cos\omega),$$

where $P_k(\cos\omega)$ is the Legendre polynomial of order $k$. We write $\langle a|V(r_{12})P_S|a'\rangle$ as

$$\langle a|V(r_{12})P_S|a'\rangle=\tfrac{1}{4}\sum_{n,k} f_{nk}F_k, \quad \text{(A2)}$$

where

$$f_{nk}=(-1)^n(2k+1)\times\langle j_1j_2JM|\boldsymbol{\sigma}_1^{(n)}\cdot\boldsymbol{\sigma}_2^{(n)}P_k(\cos\omega)|j_1'j_2'J'M'\rangle, \quad \text{(A3)}$$

[25] Y. E. Kim and J. O. Rasmussen, UCRL-10707, 1963, Nucl. Phys. (to be published).
[26] J. R. Erskine, W. W. Buechner, and H. A. Enge, Phys. Rev. 128, 720 (1962).

and

$$F_k=\frac{1}{2k+1}\int\int R_1^*(r_1)R_2^*(r_2)v_k(r_1,r_2)\times R_1'(r_1)R_2'(r_2)r_1^2r_2^2dr_1dr_2. \quad \text{(A4)}$$

By the addition theorem for spherical harmonics, we may write $P_k(\cos\omega)$ as

$$P_k(\cos\omega)=\sum_\kappa (-1)^\kappa C_\kappa^{(k)}(1)C_{-\kappa}^{(k)}(2),$$

where

$$C_\kappa^{(k)}(\theta_i)=\left[\frac{4\pi}{2k+1}\right]^{1/2}Y_\kappa^{(k)}(\theta_i,\phi_i),$$

so that

$$f_{nk}=\sum_{\kappa,\gamma}(-1)^{n+\kappa+\gamma}(2k+1)\langle j_1j_2JM|\sigma_\gamma^{(n)}(1)C_\kappa^{(k)}(1)\cdot\sigma_{-\gamma}^{(n)}(2)C_{-\kappa}^{(k)}(2)|j_1'j_2'J'M'\rangle. \quad \text{(A5)}$$

The angular part $f_{nk}$ can be evaluated by using the tensor-operator algebra developed by Racah,[27] and de-Shalit has obtained the expression of $f_{nk}$ for the diagonal case in the zero-range limit.[4] The similar expression including the off-diagonal case can be calculated easily and is given in terms of the usual 6-$j$ and 9-$j$ symbols by

$$f_{nk}=(-1)^{j_1'+j_2'+J}\delta_{J,J'}\delta_{M,M'}(2k+1)[j,j']^{1/2}(\tfrac{1}{2}\|\sigma^{(n)}\|\tfrac{1}{2})^2(l_1\|C^{(k)}\|l_1')(l_2\|C^{(k)}\|l_2')\times\sum_r(-1)^{k+r}(2r+1)\begin{Bmatrix}j_1 & j_2 & J\\ j_2' & j_1' & r\end{Bmatrix}\begin{Bmatrix}n & k & r\\ \frac{1}{2} & l_1 & j_1\\ \frac{1}{2} & l_1' & j_1'\end{Bmatrix}\begin{Bmatrix}n & k & r\\ \frac{1}{2} & l_2 & j_2\\ \frac{1}{2} & l_2' & j_2'\end{Bmatrix}, \quad \text{(A6)}$$

where

$$[j,j']=[(2j_1+1)(2j_1'+1)(2j_2+1)(2j_2'+1)],$$

and $(\frac{1}{2}\|\sigma^{(n)}\|\frac{1}{2})$ and $(l'\|C^{(k)}\|l')$ are the usual reduced matrix elements. Here the summation over $r$ is restricted by $|k-n|\leqslant r\leqslant k+n$. Obviously, we have

$$\langle a|V(\mathbf{r}_1-\mathbf{r}_2)|a'\rangle=\sum_k f_{0k}F_k,$$

$$\langle a|V(\mathbf{r}_1-\mathbf{r}_2)\boldsymbol{\sigma}_1\cdot\boldsymbol{\sigma}_2|a'\rangle=-\sum_k f_{1k}F_k, \quad \text{(A7)}$$

and

$$\langle a|V(r_{12})P_S|a'\rangle=\tfrac{1}{4}[\langle a|V(\mathbf{r}_1-\mathbf{r}_2)a'\rangle-\langle a|V(\mathbf{r}_1-\mathbf{r}_2)\boldsymbol{\sigma}_1\cdot\boldsymbol{\sigma}_2|a\rangle],$$

where $\langle a|V(r_{12})|a'\rangle$ is just the matrix element for the Wigner force ($n=0$), whereas $\langle a|V(\mathbf{r}_1-\mathbf{r}_2)\boldsymbol{\sigma}_1\cdot\boldsymbol{\sigma}_2|a'\rangle$ is the contribution from the spin-dependent force ($n=1$). Instead of evaluating $\langle a|V(r_{12})\boldsymbol{\sigma}_1\cdot\boldsymbol{\sigma}_2|a'\rangle$ directly, we shall find it easier to evaluate $\langle a|V(r_{12})P_S|a'\rangle$ first and then obtain $\langle a|V(r_{12})\boldsymbol{\sigma}_1\cdot\boldsymbol{\sigma}_2|a'\rangle$ by subtracting the contribution due to $\langle a|V(r_{12})|a'\rangle$ from $\langle a|V(r_{12})P_S|a'\rangle$.

Because $n$ can take only two values, 0 and 1, we find it convenient to sum over $n$ first. We may sum over $n$ in Eq. (A6) by using

$$\sum_y(2y+1)\begin{Bmatrix}d & q & e\\ p & c & b\\ a & f & y\end{Bmatrix}\begin{Bmatrix}h & r & e\\ s & g & b\\ a & f & y\end{Bmatrix}=\sum_x(2x+1)\begin{Bmatrix}a & b & x\\ c & d & p\end{Bmatrix}\begin{Bmatrix}c & d & x\\ e & f & q\end{Bmatrix}\begin{Bmatrix}e & f & x\\ g & h & r\end{Bmatrix}\begin{Bmatrix}g & h & x\\ a & b & s\end{Bmatrix}, \quad \text{(A8)}$$

which is easy to verify. Summation over $r$ can also be easily performed, yielding a simpler expression involving the 3-$j$ symbol:

$$\sum_n f_{nk}=(-1)^{j_1'+j_1+J+1}2(2k+1)[j,j',l,l']^{1/2}\begin{pmatrix}l_1 & l_1' & k\\ 0 & 0 & 0\end{pmatrix}\begin{pmatrix}l_2 & l_2' & k\\ 0 & 0 & 0\end{pmatrix}\begin{Bmatrix}j_1 & l_1 & \frac{1}{2}\\ l_2 & j_2 & J\end{Bmatrix}\begin{Bmatrix}\frac{1}{2} & l_2' & j_2'\\ J & j_1' & l_1'\end{Bmatrix}\begin{Bmatrix}k & l_2' & l_2\\ J & l_1 & l_1'\end{Bmatrix}. \quad \text{(A9)}$$

Here we have

$$[j,j',l,l']=[(2j_1+1)(2j_1'+1)(2j_2+1)(2j_2'+1)(2l_1+1)(2l_1'+1)(2l_2+1)(2l_2'+1)].$$

The final expression for $\langle a|V(r_{12})P_S|a'\rangle$ is

$$\langle a|V(r_{12})P_S|a'\rangle=\tfrac{1}{2}\sum_k F_k(-1)^{j_2'+j_2+J+1}[j,j',l,l'](l_10l_1'0|k0)(l_20l_2'0|k0)W(l_1j_1l_2j_2;\tfrac{1}{2}J)\times W(l_1'j_1'l_2'j_2';\tfrac{1}{2}J)W(l_1l_1'l_2l_2';kJ), \quad \text{(A10)}$$

where the symbols ( | ) and $W$ are the usual Clebsch-Gordan and Racah coefficients.

[27] G. Racah, Phys. Rev. **62**, 438 (1942).

Now we evaluate $\langle a|V(r_{12})|a'\rangle$. Noting

$$\begin{Bmatrix} 0 & k & r \\ s & l & j \\ s' & l' & j' \end{Bmatrix} = (-1)^{k+s+j+l'}[2(2k+1)]^{-1/2} \begin{Bmatrix} j' & j & k \\ l & l' & s \end{Bmatrix} \delta_{k,r},$$

we can easily verify

$$\langle a|V(r_{12})|a'\rangle = \sum_k F_k(-1)^{j_2'+j_2+J}[j,j']^{1/2}(j_1'\tfrac{1}{2}j_1-\tfrac{1}{2}|k0)(j_2'\tfrac{1}{2}j_2-\tfrac{1}{2}|k0)W(j_1j_1'j_2j_2';kJ), \quad \text{(A11)}$$

with the restriction that it vanishes unless both $l_1+l_1'+k$ and $l_2+l_2'+k$ are even. From Eqs. (A7), (A10), and (A11), we get

$$\langle a|V(r_{12})\boldsymbol{\sigma}_1\cdot\boldsymbol{\sigma}_2|a'\rangle = 2\sum_k F_k(-1)^{j_2+j_2'+J}[j,j',l,l']^{1/2}(l_10l_1'0|k0)(l_20l_2'0|k0)W(l_1j_1l_2j_2;\tfrac{1}{2}J)$$
$$\times W(l_1'j_1'l_2'j_2';\tfrac{1}{2}J)W(l_1l_1'l_2l_2';kJ)+\langle a|V(r_{12})|a'\rangle, \quad \text{(A12)}$$

where $\langle a|V(r_{12})|a'\rangle$ is given by Eq. (A11).

Now that we have obtained the explicit forms of the spin-dependent matrix element for the finite-range case, we obtain the corresponding expressions in the limit of zero range. For the zero-range force, we have $F_k \equiv F_0$ for every $k$, so that the summation over $k$ can be easily carried out analytically. The final results for the zero-range force are

$$\langle a|V^0(r_{12})|a'\rangle = \frac{1}{2(2J+1)}F_0[j,j']^{1/2}(j_1\tfrac{1}{2}j_2-\tfrac{1}{2}|J0)(j_1'\tfrac{1}{2}j_2'-\tfrac{1}{2}|J0)$$
$$\times\left[(-1)^{j_1+j_1'+l_1+l_1'+1}+(-1)^{j_1+j_1'+j_2+j_2'}\frac{AA'}{4J(J+1)}\right] \quad \text{(A13)}$$

and

$$\langle a|V^0(r_{12})\boldsymbol{\sigma}_1\cdot\boldsymbol{\sigma}_2|a'\rangle = \frac{1}{2(2J+1)}F_0[j,j']^{1/2}(j_1\tfrac{1}{2}j_2-\tfrac{1}{2}|J0)(j_1'\tfrac{1}{2}j_2'-\tfrac{1}{2}|J0)$$
$$\times\left\{(-1)^{j_1+j_1'+l_1+l_1'}[1+2(-1)^{l_1+l_2+J}]+(-1)^{j_1+j_1'+j_2+j_2'}\frac{AA'}{4J(J+1)}\right\}, \quad \text{(A14)}$$

where the superscript zero refers to the zero-range limit, and

$$A=(2j_1+1)+(-1)^{j_1+j_2+J}(2j_2+1).$$

In Eq. (A13), $\langle a|V^0(r_{12})|a'\rangle$ vanishes unless $l_1+l_1'+l_2+l_2'$ is even. Likewise, $\langle a|V^0(r_{12})\boldsymbol{\sigma}_1\cdot\boldsymbol{\sigma}_2|a'\rangle$ vanishes unless both $l_1+l_2+J$ and $l_1'+l_2'+J$ are even. The diagonal cases of both Eqs. (13) and (14) agree with the results obtained by de-Shalit.[4] An almost identical expression for (A13) is given by Newby and Konopinski,[6] and a similar expression by Noya *et al.*[10] Equations (A10) and (A11) are also given by Newby and Konopinski.

## APPENDIX B

The tensor-force matrix element will be evaluated here in the $j$-$j$ representation. We may express the tensor force in terms of the orbital and spin tensors as

$$\tfrac{1}{3}V(r_{12})S_{12}=(\mathbf{S}^{(2)}\cdot\mathbf{L}^{(2)}),$$

where $\mathbf{S}^{(2)}$ is the irreducible tensor operator of rank 2 constructed from the spin operators $\boldsymbol{\sigma}_1$ and $\boldsymbol{\sigma}_2$, and $\mathbf{L}^{(2)}$ is a product of the scalar $V(r_{12})$ and the irreducible operator of rank 2 constructed from the unit vector $\mathbf{r}_{12}/r_{12}$. The spin and orbital tensors may be obtained from[28]

$$S_m^{(2)}=(8\pi/15)^{1/2}(\boldsymbol{\sigma}_1\cdot\nabla)(\boldsymbol{\sigma}_2\cdot\nabla)\mathcal{Y}_{2m}(\mathbf{r}_{12})$$
$$L_m^{(2)}=\left(\frac{2\pi}{15}\right)^{1/2}\frac{V(r_{12})}{r_{12}^2}\mathcal{Y}_{2m}(\mathbf{r}_{12}),$$

where $\mathcal{Y}_{lm}(\mathbf{r})=r^lY_{lm}(\theta,\phi)$ and $Y(\theta,\phi)$ is the spherical harmonics.

The tensor force have been evaluated into spherical tensors by Talmi.[29] Expanding $V(r_{12})/r_{12}^2$ in terms of spherical harmonics,

$$V(r_{12})/r_{12}^2=\sum_k v_k(r_1,r_2)P_k(\cos\omega_{12})$$
$$=\sum_{k=0}^{\infty}v_k(r_1,r_2)\sum_\kappa(-1)^\kappa C_\kappa^{(k)}(1)C_{-\kappa}^{(k)}(2),$$

we obtain for the tensor force in terms of spherical

[28] A. R. Edmonds, *Angular Momentum in Quantum Mechanics* (Princeton University Press, Princeton, 1957).
[29] I. Talmi, Phys. Rev. 89, 1065 (1953).

tensors

$$V(r_{12})S_{12}=3\sum_{K,x,y}F_{xy}W(1x1y;K2)\mathbf{T}_1^{(1x)K}\cdot\mathbf{T}_2^{(1y)K},$$

where

$$F_{xy}=-5\sum v_k(r_1,r_2)\{(2/15)^{1/2}[x]^{1/2}(20k0|x0)r_1^2+(2/15)^{1/2}[y]^{1/2}(20k0|y0)r_2^2+([x][y])^{1/2}(10k0|x0)(10k0|y0)W(11xy;2k)r_1r_2\},$$

and

$$\mathbf{T}_i^{(1z)K}=[\boldsymbol{\sigma}^{(1)}(i)\times\mathbf{C}^{(z)}(i)]\quad\text{for}\quad i=1\text{ or }2.$$

The symbols ( | ) and $W$ are the usual Clebsch-Gordan and Racah coefficients, and $[a]$ stands for $[2a+1]$. Now the evaluation of the matrix element for $V(r_{12})S_{12}$ is straightforward by using the similar method of Appendix A. The final result is

$$\langle a|V(r_{12})S_{12}|a'\rangle=3\sum_{K,x,y}\langle\alpha|F_{xy}|\alpha'\rangle W(1x1y;K2)\times\langle j_1j_2JM|\mathbf{T}_1^{(1x)K}\cdot\mathbf{T}_2^{(1y)K}|j_1'j_2'J'M'\rangle,$$

where

$$\langle\alpha|F_{xy}|\alpha'\rangle=-5\sum_{k,i,j}\langle\alpha|r_ir_j|\alpha'\rangle X_{ij}\quad\text{for}\quad i,j=1,2,$$

$$X_{11}=(2/15)^{1/2}[x]^{1/2}(20k0|x0),$$

$$X_{22}=(2/15)^{1/2}[y]^{1/2}(20k0|y0),$$

$$X_{12}=([x][y])^{1/2}(10k0|x0)(10k0|y0)\times W(11xy;2k),$$

and

$$\langle\alpha|r_ir_j|\alpha'\rangle=(2k+1)\int_0^\infty dr_1\,r_1^2R_1R_1'\int_0^\infty dr_2r_2^2R_2R_2'r_ir_j\times\int_{-1}^{1}d\left(\frac{\cos\omega_{12}}{2}\right)P_k(\cos\omega_{12})\frac{V(r_{12})}{r_{12}^2}.$$

The angular part is given in terms of 3-, 6-, and 9-$j$ symbols as

$$\langle j_1j_2JM|\mathbf{T}_1^{(1x)K}\cdot\mathbf{T}_2^{(1y)K}|j_1'j_2'J'M'\rangle=(-1)^{j_1'+j_2+l_1+l_2+J}6\delta_{JJ'}\delta_{MM'}\begin{Bmatrix}J&j_2&j_1\\k&j_1'&j_2'\end{Bmatrix}([j_1][j_2][j_1'][j_2'])^{1/2}\times([l_1][l_2][l_1'][l_2'])^{1/2}\begin{pmatrix}l_1&x&l_1'\\0&0&0\end{pmatrix}\begin{pmatrix}l_2&y&l_2'\\0&0&0\end{pmatrix}\begin{Bmatrix}\frac12&\frac12&1\\l_1'&l_1&x\\j_1'&j_1&K\end{Bmatrix}\begin{Bmatrix}\frac12&\frac12&1\\l_2'&l_2&y\\j_2'&j_2&K\end{Bmatrix}.$$

An almost identical result for the diagonal case only is given by de-Shalit and Walecka.[23] The radial integral $\langle\alpha|r_ir_j|\alpha'\rangle$ can be evaluated by expanding it into a linear combination of Talmi integrals

$$\langle\alpha|r_ir_j|\alpha'\rangle=\sum_{m,m'}f_k(m,m')=\sum_{m,m'}(1/2\pi)^{1/2}2^{-(m+m')-3}\times\sum_\sigma(m+m'-2\sigma+1)!!T_k^{2\sigma}(m,m')J_{2\sigma},$$

where $f_k$ is the double integral of the form

$$f_k=\int\int x_1^m x_2^{m'}v_k(r_1,r_2)\exp(-x_1^2-x_2^2)x_1^2dx_1x_2^2dx_2.$$

The variable $x_i$ is defined here as $r_i/\sqrt{\nu}$ and $(\nu)^{-1/2}$ is the length parameter appearing in the harmonic oscillator radial wave functions, and

$$v_k(r_1,r_2)=(2k+1)\int_{-1}^{1}d\left(\frac{\cos\omega_{12}}{2}\right)P_k(\cos\omega_{12})\frac{V(r_{12})}{r_{12}^2}.$$

The Talmi integral $J_{2\sigma}$ is the single integral defined as

$$J_{2\sigma}=\int_0^\infty x^{2\sigma}\exp\left(-\frac{x^2}{2}\right)\frac{V(\nu^{1/2}x)}{\nu x^2}x^2dx.$$

The expansion coefficient, $T$, is the Talmi coefficient defined by Ford and Konopinski,[16] and the explicit expressions along with several recursion relations for the Talmi coefficients are given in detail by Ford and Konopinski.